

Synthesis and Lithium Fast-Ion Conductivity of a New Complex Hydride $\text{Li}_3(\text{NH}_2)_2\text{I}$ with Double-Layered Structure

Motoaki Matsuo,[†] Toyoto Sato,[‡] Yohei Miura,[†]
Hiroyuki Oguchi,^{†,§} Yu Zhou,[†] Hideki Maekawa,[§]
Hitoshi Takamura,[§] and Shin-ichi Orimo^{*,†}

[†]Institute for Materials Research, Tohoku University,
Katahira 2-1-1, Sendai 980-8577, Japan, [‡]WPI Advanced
Institute for Materials Research, Tohoku University, Katahira
2-1-1, Sendai 980-8577, Japan, and [§]Graduate School of
Engineering, Tohoku University, Aramaki Aza Aoba 6-6-02,
Sendai 980-8579, Japan

Received March 6, 2010
Revised Manuscript Received April 12, 2010

We have recently reported that a complex hydride $\text{Li}(\text{BH}_4)$, a potential candidate for advanced hydrogen storage materials,¹ exhibits lithium fast-ion conduction.² The ion conductivity of $\text{Li}(\text{BH}_4)$ increases by 3 orders of magnitude at approximately 390 K due to its structural transition from the orthorhombic low-temperature phase to the hexagonal high-temperature phase. No complex hydride except $\text{Li}(\text{BH}_4)$ has been reported to exhibit lithium fast-ion conduction since the report of $\text{Li}_2(\text{NH})$ in 1979,³ although a wide variety of inorganic lithium fast-ion conductors such as oxides^{4–7} and sulfides^{8–11} have been studied. Research and development of lithium (fast-)ion conductors is significantly important because they can be potentially used as solid electrolytes in all-solid-state lithium ion batteries.¹² From the application point of view, it is highly desirable to enhance the conductivity of $\text{Li}(\text{BH}_4)$ at room temperature (RT).

Recently, the enhanced conductivities in the $\text{Li}(\text{BH}_4)\text{--LiX}$ ($\text{X} = \text{Cl}, \text{Br}, \text{and I}$)¹³ and $\text{Li}(\text{BH}_4)\text{--Li}(\text{NH}_2)$ ¹⁴ systems have been demonstrated. In the $\text{Li}(\text{BH}_4)\text{--LiI}$ system (Figure 1), the high-temperature phase of $\text{Li}(\text{BH}_4)$ can be stabilized at lower temperature (below 390 K) by forming solid solution phase with a wide range of compositions; as a result, the conductivity (4×10^{-5} S/cm) becomes 3 orders of magnitude higher than that of pure $\text{Li}(\text{BH}_4)$ (2×10^{-8} S/cm) at RT. LiCl also partially dissolves into $\text{Li}(\text{BH}_4)$, resulting in the stabilization of the high-temperature phase.^{13,15} In the case of the $\text{Li}(\text{BH}_4)\text{--Li}(\text{NH}_2)$ system (Figure 1), two stoichiometric compounds, $\text{Li}_2(\text{BH}_4)(\text{NH}_2)$ and $\text{Li}_4(\text{BH}_4)(\text{NH}_2)_3$, both with combinations of $(\text{BH}_4)^-$ and $(\text{NH}_2)^-$ complex anions, show fast-ion conductivities of 1×10^{-4} S/cm at RT because of new occupation sites available to Li^+ ions. These experimental results suggest that various fast-ion conductors may exist in the $\text{Li}(\text{BH}_4)\text{--Li}(\text{NH}_2)\text{--LiI}$ system. It is important to study the material properties of the $\text{Li}(\text{NH}_2)\text{--LiI}$ system before studying the $\text{Li}(\text{BH}_4)\text{--Li}(\text{NH}_2)\text{--LiI}$ system.

Here we report the synthesis and the lithium fast-ion conductivity of the new complex hydride $\text{Li}_3(\text{NH}_2)_2\text{I}$ found in the $\text{Li}(\text{NH}_2)\text{--LiI}$ system. Structural analysis based on high-resolution synchrotron X-ray diffraction shows that $\text{Li}_3(\text{NH}_2)_2\text{I}$ has the characteristic double-layered structure constructed by the clusters composed of six $(\text{NH}_2)_3\text{I}$ tetrahedra. Because of the unique crystal structure, $\text{Li}_3(\text{NH}_2)_2\text{I}$ exhibits fast-ion conductivity of 1×10^{-5} S/cm at RT with a lithium ion transport number of almost unity.

Powder X-ray diffraction was performed for $(1 - x)\text{Li}(\text{NH}_2) + x\text{LiI}$ ($x = 0.06\text{--}0.75$), synthesized by mechanical milling and subsequent heat treatment for the sufficient crystal growth, by Cu $K\alpha$ characteristic radiation using the laboratory X-ray apparatus (Lab-XRD) at RT, and the results are shown in Figure 2a. Even for the low LiI composition ratio ($x = 0.06$), the diffraction peaks of a new phase are clearly observed along with the starting material $\text{Li}(\text{NH}_2)$. The peak intensities of $\text{Li}(\text{NH}_2)$ decrease as x increases, and only the new phase is detected for $x = 0.25$. With further increase in x , the peaks of LiI appear in turn. Other peaks originating from related compounds such as $\text{Li}_2(\text{NH})$ or Li_3N are not observed. The peak positions of the new phase do not shift over the whole range of composition ratios. From these results, at this point, we deduce that the new phase may be the

- (1) Orimo, S.; Nakamori, Y.; Eliseo, J. R.; Züttel, A.; Jensen, C. M. *Chem. Rev.* **2007**, *107*, 4111.
- (2) Matsuo, M.; Nakamori, Y.; Orimo, S.; Maekawa, H.; Takamura, H. *Appl. Phys. Lett.* **2007**, *91*, 224103.
- (3) Boukamp, B. A.; Huggins, R. A. *Phys. Lett. A* **1979**, *72*, 464.
- (4) Aono, H.; Sugimoto, E.; Sadaoka, Y.; Imanaka, N.; Adachi, G. *J. Electrochem. Soc.* **1993**, *140*, 1827.
- (5) Inaguma, Y.; Liqun, C.; Itoh, M.; Nakamura, T.; Uchida, T.; Ikuta, H.; Wakihara, M. *Solid State Commun.* **1993**, *86*, 689.
- (6) Martínez-Juárez, A.; Rojo, J. M.; Iglesias, J. E.; Sanz, J. *Chem. Mater.* **1995**, *7*, 1857.
- (7) Thangadurai, V.; Shukla, A. K.; Gopalakrishnan, J. *Chem. Mater.* **1999**, *11*, 835.
- (8) Tachez, M.; Malugani, J. P.; Mercier, R.; Robert, G. *Solid State Ionics* **1984**, *14*, 181.
- (9) Sahami, S.; Shea, S. W.; Kennedy, J. H. *J. Electrochem. Soc.* **1985**, *132*, 985.
- (10) Kanno, R.; Murayama, M. *J. Electrochem. Soc.* **2001**, *148*, A742.
- (11) Ito, K.; Hayashi, A.; Morimoto, H.; Tatsumisago, M.; Minami, T. *Chem. Mater.* **2002**, *14*, 2444.
- (12) Ohta, N.; Takada, K.; Zhang, L.; Ma, R.; Osada, M.; Sasaki, T. *Adv. Mater.* **2006**, *18*, 2226.
- (13) (a) Matsuo, M.; Takamura, H.; Maekawa, H.; Li, H. -W.; Orimo, S. *Appl. Phys. Lett.* **2009**, *94*, 084103. (b) Maekawa, H.; Matsuo, M.; Takamura, H.; Ando, M.; Noda, Y.; Karahashi, T.; Orimo, S. *J. Am. Chem. Soc.* **2009**, *131*, 894. (c) Oguchi, H.; Matsuo, M.; Hummelshøj, J. S.; Vegge, T.; Nørskov, J. K.; Sato, T.; Miura, Y.; Takamura, H.; Maekawa, H.; Orimo, S. *Appl. Phys. Lett.* **2009**, *94*, 141912.

- (14) Matsuo, M.; Remhof, A.; Martelli, P.; Caputo, R.; Ernst, M.; Miura, Y.; Sato, T.; Oguchi, H.; Maekawa, H.; Takamura, H.; Borgschulte, A.; Züttel, A.; Orimo, S. *J. Am. Chem. Soc.* **2009**, *131*, 16389.
- (15) (a) Mosegaard, L.; Møller, B.; Jørgensen, J. E.; Filinchuk, Y.; Cerenius, Y.; Hanson, J. C.; Dimasi, E.; Besenbacher, F.; Jensen, T. R. *J. Phys. Chem. C* **2008**, *112*, 1299. (b) Arnbjerg, L. M.; Ravnsbæk, D. B.; Filinchuk, Y.; Vang, R. T.; Cerenius, Y.; Besenbacher, F.; Jørgensen, J. E.; Jakobsen, H. J.; Jensen, T. R. *Chem. Mater.* **2009**, *21*, 5772.

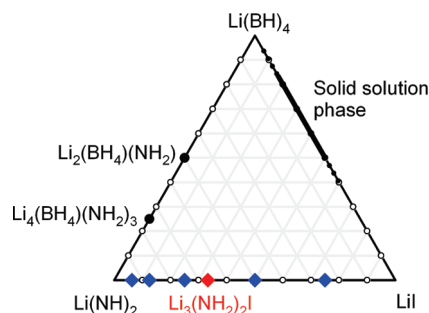


Figure 1. Schematic phase diagram of the $\text{Li}(\text{BH}_4)$ – $\text{Li}(\text{NH}_2)$ – LiI system. Diamonds in the $\text{Li}(\text{NH}_2)$ – LiI system are compositions synthesized, and $\text{Li}_3(\text{NH}_2)_2\text{I}$ is the new complex hydride found in this study.

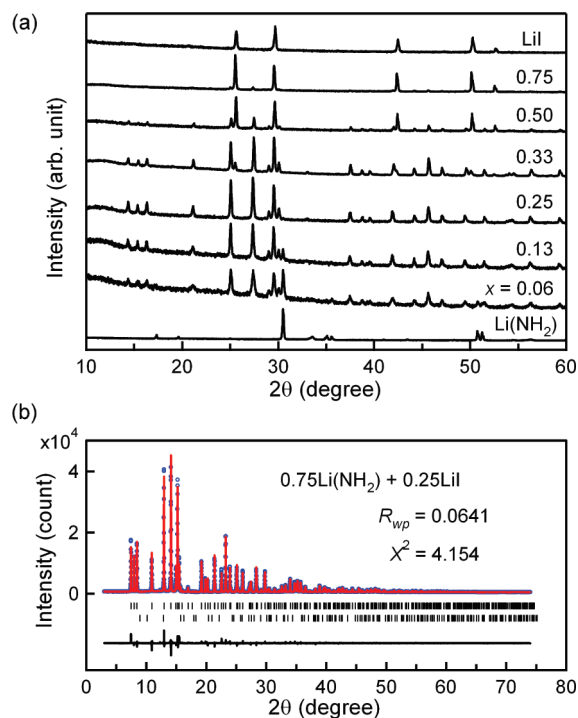


Figure 2. (a) Lab-XRD profiles of $(1-x)\text{Li}(\text{NH}_2) + x\text{LiI}$ ($x = 0.06$ – 0.75). For reference, the data of $\text{Li}(\text{NH}_2)$ and LiI as host materials are also shown. (b) Rietveld refinement fits of SR-XRD for $0.75\text{Li}(\text{NH}_2) + 0.25\text{LiI}$. The observed, calculated, and difference between observed and calculated profiles are indicated blue circles, a red line, and a black line, respectively. The positions of Bragg reflection are shown for $\text{Li}_3(\text{NH}_2)_2\text{I}$ (upper) and $\text{Li}(\text{NH}_2)$ (lower).

stoichiometric compound “ $\text{Li}_4\text{N}_3\text{H}_6\text{I}$ ” ($0.75\text{Li}(\text{NH}_2) + 0.25\text{LiI} \rightarrow 0.25\text{Li}_4\text{N}_3\text{H}_6\text{I}$).

To determine the crystal structure of the new phase, a high-resolution synchrotron powder X-ray diffraction experiment was carried out for $x = 0.25$ at RT (SR-XRD, $\lambda = 0.8006 \text{ \AA}$). The Rietveld refinement fit of SR-XRD for the new phase is shown in Figure 2b (the details of structure determination are described in the Supporting Information). The Rietveld refinement reveals small peaks of unreacted $\text{Li}(\text{NH}_2)$; further, the true composition of the new phase is found to be $\text{Li}_3(\text{NH}_2)_2\text{I}$ with $a = 7.09109(5) \text{ \AA}$, $c = 11.50958(10) \text{ \AA}$, the space group $P6_3mc$ (hexagonal), and $Z = 4$. The refined molar ratio of $\text{Li}_3(\text{NH}_2)_2\text{I}$: $\text{Li}(\text{NH}_2)$ is determined to be 1.4:1. This result agrees reasonably with the theoretical optimal ratio of 1:1 obtained from the following equation: $0.75\text{Li}(\text{NH}_2) + 0.25\text{LiI} \rightarrow 0.25(\text{Li}_3(\text{NH}_2)_2\text{I} + \text{Li}(\text{NH}_2))$.

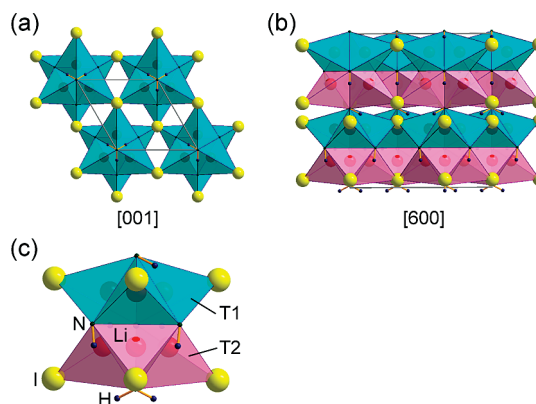


Figure 3. Crystal structure of the new complex hydride $\text{Li}_3(\text{NH}_2)_2\text{I}$ viewed along (a) $[001]$ and (b) $[600]$ and (c) cluster composed of six tetrahedra. T1 and T2 indicate tetrahedra composed of three N atoms and one I atom for Li1 and Li2, respectively.

Nevertheless, the single-phase $\text{Li}_3(\text{NH}_2)_2\text{I}$ was not obtained for $x = 0.33$ ($0.67\text{Li}(\text{NH}_2) + 0.33\text{LiI} \rightarrow 0.33\text{Li}_3(\text{NH}_2)_2\text{I}$) as shown in Figure 2a, which might be due to the small amount of hydrogen desorption, less than 0.5 wt % confirmed by hydrogen analysis, during the heat treatment process.

The crystal structure of $\text{Li}_3(\text{NH}_2)_2\text{I}$ is illustrated in Figure 3. The Li atoms are located at two crystallographically different positions (Li1 and Li2). Both the Li1 and the Li2 atoms are tetrahedrally coordinated by three N atoms and one I atom (tetrahedra T1 for Li1 and T2 for Li2). The main feature of the structure is the clusters composed of three T1 and three T2 tetrahedra that share their edges with each other (Figure 3c). The double-layered structure consists of the corner-shared clusters such that the upper layer makes an angle of 60° with the lower (Figure 3a,b).

To investigate the electrical conductivity of $\text{Li}_3(\text{NH}_2)_2\text{I}$, ac impedance measurements were performed for the pelletized powders of $(1-x)\text{Li}(\text{NH}_2) + x\text{LiI}$ ($x = 0.06$ – 0.75). Figure 4a shows the typical impedance plot for $x = 0.25$ obtained by using a pair of lithium electrodes. The plot shows two overlapping high- and low-frequency arcs, indicating that the responses arise from both the bulk (capacitance (C): 100–300 pF) and grain boundary (C : 20–50 nF),^{2,13} which is probably related to a weak adhesion force of the particles in the pelletized sample (see Figure S2 in the Supporting Information). Figure 4b shows the temperature dependence of the conductivity for $x = 0.25$ calculated from the intercept of the low-frequency arc. As shown in the inset of Figure 4b, the maximum conductivity of $1.7 \times 10^{-5} \text{ S/cm}$ at 300 K, which is four and three orders of magnitude higher than that of the host materials $\text{Li}(\text{NH}_2)$ and LiI ,¹⁶ respectively, is obtained for $x = 0.25$ of all compositions, although almost equimolar $\text{Li}(\text{NH}_2)$ exists in the sample. This result implies that higher conductivity can be achieved for the single-phase $\text{Li}_3(\text{NH}_2)_2\text{I}$. The activation energy for conduction is evaluated to be 0.58 eV, comparable to that of the high-temperature phase of $\text{Li}(\text{BH}_4)$ (0.53 eV).² Lab-XRD analysis revealed

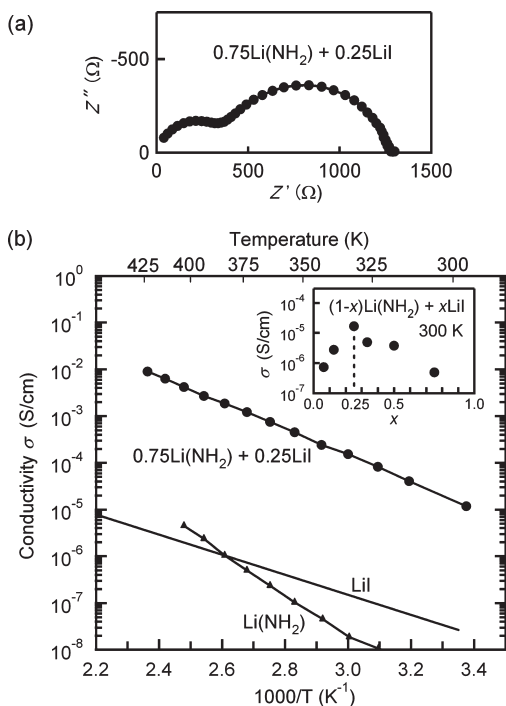


Figure 4. Electrical properties of $0.75\text{Li}(\text{NH}_2) + 0.25\text{LiI}$. (a) A typical impedance plot obtained using a lithium electrode at 313 K. (b) Temperature dependence of the electrical conductivity. For reference, the data of $\text{Li}(\text{NH}_2)$ and LiI^{16} as host materials are also shown. The inset shows the conductivities of $(1-x)\text{Li}(\text{NH}_2) + x\text{LiI}$ at 300 K.

that no significant changes occurred at the interface between the complex hydrides and the lithium electrode before and after the ac impedance measurements (see Figure S3 in the Supporting Information).

The dc conductivity was also measured using blocking and nonblocking electrodes to determine the lithium ion transport number of $\text{Li}_3(\text{NH}_2)_2\text{I}$. Figure 5 shows the dc conductivity of $0.75\text{Li}(\text{NH}_2) + 0.25\text{LiI}$ at 296 K as a function of time. When lithium (nonblocking) electrodes are used, the dc conductivity remains almost constant with time; the conductivity is around 1×10^{-5} S/cm, which agrees well with the value obtained from ac impedance measurements, shown in Figure 4b. On the other hand, when the molybdenum (blocking) electrodes are used, the conductivity initially decreases with time and then becomes almost constant, and the value is about 4 orders of magnitude lower than that obtained using the lithium electrodes. These results indicate that the electronic conduction is almost negligible. Thus, the new complex hydride $\text{Li}_3(\text{NH}_2)_2\text{I}$, shown in Figure 3, is a pure lithium ion conductor.

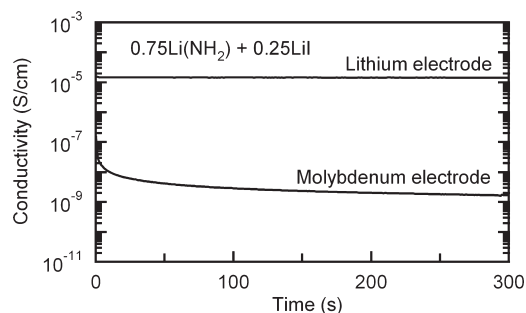


Figure 5. Time dependence of dc conductivity of $0.75\text{Li}(\text{NH}_2) + 0.25\text{LiI}$ after applying a constant voltage of 0.1 V for lithium (nonblocking) or molybdenum (blocking) electrodes at 296 K.

The lithium fast-ion conduction of $\text{Li}_3(\text{NH}_2)_2\text{I}$ may be closely related to the unique crystal structure. As shown in Figure 3, there are many intrinsic vacancies at the center of the cluster composed of six tetrahedra and between the clusters. Li^+ ions may migrate through these vacancies. A detailed study using high-resolution NMR and neutron diffraction/scattering is highly desired. Higher conductivity will be achieved by the anion substitution as demonstrated in the $\text{Li}(\text{BH}_4)\text{--Li}(\text{NH}_2)$ system.¹⁴

In summary, we have succeeded in synthesizing the new complex hydride $\text{Li}_3(\text{NH}_2)_2\text{I}$ exhibiting lithium fast-ion conductivity. Structural analysis based on high-resolution synchrotron X-ray diffraction shows that $\text{Li}_3(\text{NH}_2)_2\text{I}$ has the characteristic double-layered structure with $a = 7.09109(5)$ Å, $c = 11.50958(10)$ Å, the space group $P6_3mc$ (hexagonal), and $Z = 4$. Because of the characteristic structure, $\text{Li}_3(\text{NH}_2)_2\text{I}$ exhibits fast-ion conductivity of 1×10^{-5} S/cm at 296 K with a lithium ion transport number of almost unity, although the conductivities of the host materials $\text{Li}(\text{NH}_2)$ (3×10^{-9} S/cm) and LiI (3×10^{-8} S/cm) are very low.

Acknowledgment. We thank Dr. M. Takata, Dr. J. Kim, and Dr. N. Tsuji, Japan Synchrotron Radiation Research Institute, for their technical support for the SR-XRD measurement. This work was partially supported by MEXT, Japan (Global COE Program “Materials Integration, Tohoku University” and KAKENHI (18GS0203 and 21246100)) and NEDO, Japan (Advanced Fundamental Research Project on Hydrogen Storage Materials).

Supporting Information Available: X-ray crystallographic file (CIF). Experimental and structural determination procedures, microstructure analysis, and XRD data (PDF). This material is available free of charge via the Internet at <http://pubs.acs.org>.